Journal of Electromyography and Kinesiology 88 (2026) 103157

Contents lists available at ScienceDirect

Journal of Electromyography and Kinesiology

journal homepage: www.elsevier.com/locate/jelekin

Congruency of fatigue-mediated changes in shear wave velocity, upper limb force, muscle activity, and kinematics of the scapular stabilizer muscles

Matthew S. Russell, Janessa D.M. Drake, Jaclyn N. Chopp-Hurley *

School of Kinesiology and Health Science, York University, Toronto, Canada

ARTICLE INFO

Keywords:
Ultrasound
Stiffness
Shoulder
Fatigue

ABSTRACT

Ultrasonographic shear wave elastography is a new technique for assessing muscle stiffness *in vivo*. Such insights may be valuable to uncover fatigue-mediated muscle stiffness and control changes at the shoulder, for which much variability remains unexplained through EMG-based methods. This study assessed fatigue-mediated changes in shear wave velocity (SWV), EMG root-mean-squared (RMS) amplitude, EMG mean-power-frequency (MdPF), and force output from upper trapezius, middle trapezius, lower trapezius, and serratus anterior, to determine whether SWV may provide a significant predictive variance in the quantification of muscle fatigue and fatigue-mediated scapulothoracic kinematics changes. 15 males and 15 females had their scapular stabilizer muscles and scapulothoracic kinematics assessed before and after a targeted muscle fatigue protocol. Results indicate that EMG RMS amplitude and EMG MdPF were most sensitive to fatigue-mediated changes at 100% contraction intensity, while SWV appeared most sensitive at 30% and 50% contraction intensity. Scapulothoracic kinematics changes appeared most sensitive to fatigue-mediated EMG MdPF changes. These results suggest that EMG MdPF changes may be elusive in a highly redundant muscular system like the shoulder due to its association with kinematics changes altering load-sharing strategies. SWV increases at contraction intensities ≤ 50% suggest post-exercise muscle edema is a likely physiological mechanism.

1. Introduction

Ultrasonographic shear wave velocity (SWV) may uniquely characterize important viscoelastic (passive) effects of muscle loading and fatigue. Unlike traditional neuromechanical fatigue indices like electromyography (EMG) and force decrement (elicited voluntarily or through tetanic stimulation) which characterize active or contractile muscle properties [Allen et al., 2008], SWV assessments of muscle stiffness characterize passive or non-contractile muscle element changes [Zimmer et al., 2023]. Decreases in SWV, thought to derive from increased viscoelastic compliance of musculotendinous tissue, have been demonstrated in resting muscle during and up to 48 h following consistent or repetitive loading [Andonian et al., 2016; Siracusa et al., 2019; Vatovec et al., 2022]. These decreases are hypothesized to reflect viscoelastic compliance due to mechanical creep, lengthening the time for muscle forces to transfer to bone and reducing the ability to store energy elastically [Kubo et al., 2001; Zimmer et al., 2023]. As such, muscle stiffness presents a hypothetical framework for disrupting muscle force and force transmission through a physiological pathway that is distinct from traditional EMG-based metrics which may supply a unique variance in fatigue-mediated muscle recruitment and control.

During muscle contraction, fatigue-mediated muscle stiffness and proportional SWV appear linearly related to joint torque changes in constrained biomechanical systems (e.g. elbow). Researchers studying the relationship between muscle stiffness, joint torque, and EMG in the elbow flexor muscles have demonstrated that stiffness relates to joint torque during submaximal contraction intensities, with force-SWV coefficient of determination values ranging from 0.85 to 0.93 across the elbow flexor muscles during a ramped-intensity isometric elbow flexion task [Bouillard et al., 2012]. Previously, the same authors reported that joint torque was better predicted by muscle stiffness ($r^2 = 0.98$–0.99) than EMG amplitude ($r^2 = 0.95$–0.97) in the abductor digiti minimi and first dorsal interosseous [Bouillard et al., 2011]. Further literature supports this notion that joint torque is better predicted by muscle stiffness or SWV than by EMG amplitude across other muscles [Yoshitake et al., 2014; Zimmer et al., 2023]. Taken together, authors surmise the variance in SWV relationships with muscle activity are mediated by the variance in force generating capacity within a

* Corresponding author at: School of Kinesiology and Health Science, York University, 4700 Keele Street, Toronto, Ontario, CA, M3J 1P3, Canada
E-mail address: jnhurley@yorku.ca (J.N. Chopp-Hurley).

https://doi.org/10.1016/j.jelekin.2026.103157
Received 24 June 2025; Received in revised form 6 April 2026; Accepted 9 April 2026
Available online 9 April 2026

population [Yoshitake et al., 2014; Mendes et al., 2018; Cipriano et al., 2022], and SWV and EMG amplitude relationships may be a reflection of load-sharing synergies preferentially recruiting muscles with higher stiffness. Yet it is currently unclear how fatigue-mediated stiffness changes might alter this muscle recruitment strategy, particularly in systems abundant with feasible muscular solutions. Such findings may have important implications for fatigue-mediated muscle recruitment in redundant muscular systems (e.g. the shoulder, postural maintenance), for which SWV may offer insight. Despite this, while a few studies have previously investigated SWV changes following exercise or muscle fatigue [Bouillard et al., 2012; Andonian et al., 2016; Siracusa et al., 2019; Vatovec et al., 2022], to date no analysis of fatigue-mediated SWV change has been reported and compared with traditional neuromuscular fatigue metrics.

Highly variable inter-individual and intra-individual kinematic and muscle activity responses to fatiguing stimuli have been demonstrated in the upper limb [Ebaugh et al., 2006; Chopp-Hurley et al., 2016; Russell et al., 2024], thought to be a product of muscular redundancy. Central to shoulder kinematic control, in particular scapular kinematics, is the muscle activity of the scapular stabilizer muscles – notably the upper trapezius (UT), middle trapezius (MT), lower trapezius (LT), and serratus anterior (SA) – which manipulate the scapula to permit shoulder elevation [Phadke et al., 2009], and have previously been implicated in variable fatigue-mediated altered control schemes [Szucs et al., 2009; Chopp et al., 2011; Noguchi et al., 2013; Russell et al., 2024]. Attempts to explain this considerable variability may benefit from an examination of fatigue-mediated muscle stiffness changes, for which this study is the first to report. Thus, the purposes of this study were to determine whether (1) fatigue-mediated changes in muscle stiffness, as measured using ultrasound shear wave elastography, are present following a targeted fatigue task of the scapular stabilizer muscles, and (2) fatigue-related changes in SWV explain a significant amount of variation in fatigue-related scapulothoracic kinematic changes. It is hypothesized that (1) muscle SWV, proportional to muscle stiffness, will decrease following a muscle fatigue protocol to reflect viscoelastic creep and hysteresis effects on fatigue-mediated reductions in muscle force [Kubo et al., 2001; Siracusa et al., 2019], and (2) fatigue-related changes in muscle SWV are expected to explain significant variance in fatigue-related scapular kinematic changes.

2. Methods

2.1. Participants

Fifteen male (27.5 ± 4.7 y; 25.3 ± 3.1 kg/m^2) and fifteen female (23.7 ± 2.7 y; 20.0 ± 1.6 kg/m^2) participants were recruited for a single 2-hour collection. From a previous study of fatigue-mediated scapular kinematics changes [Chopp et al., 2011], an *a priori* sample size of n = 30 was calculated ($\alpha = 0.05$, $\beta = 0.1$) (G*Power ver. 3.1.9.6) [Faul et al., 2007]. Participants were all self-identified as right-hand dominant although this was not an inclusion criterion. Participants were excluded if they scored below 25 on the Disabilities of the Arm, Shoulder, and Hand (DASH) [Alcántara-Bumbiedro, et al., 2006], or a score below 20 on the Tampa Scale for Kinesiophobia (TSK) [Chimenti, et al., 2021].

2.2. Data acquisition and analysis

2.2.1. Surface electromyography

Muscle activity of UT, MT, LT, and SA was collected from the dominant right side of all participants using a Delsys Trigno system (Delsys Inc., Natick, MA, USA) and surface Avanti electrodes. Signals were recorded at 2148 Hz within a passband of 20–450 Hz. (See Fig. 1.)

2.2.2. Ultrasonographic shear wave velocity

Ultrasonographic SWV measurements were captured from UT, MT, LT, and SA using a LOGIQ P9 ultrasound system (General Electric HealthCare, Mississauga, ON, Canada). Several previous studies have described optimal ultrasound transducer placement in parallel with muscle fibre orientation, approximated to the middle one-third of the muscle belly [Kelly et al., 2018]. In the present study, EMG sensor placement was prioritized to the recommended area, while ultrasound transducer location was consistently localized 2 cm superior to the recommended area, such that it was immediately superior to the EMG electrode (Fig. 2).

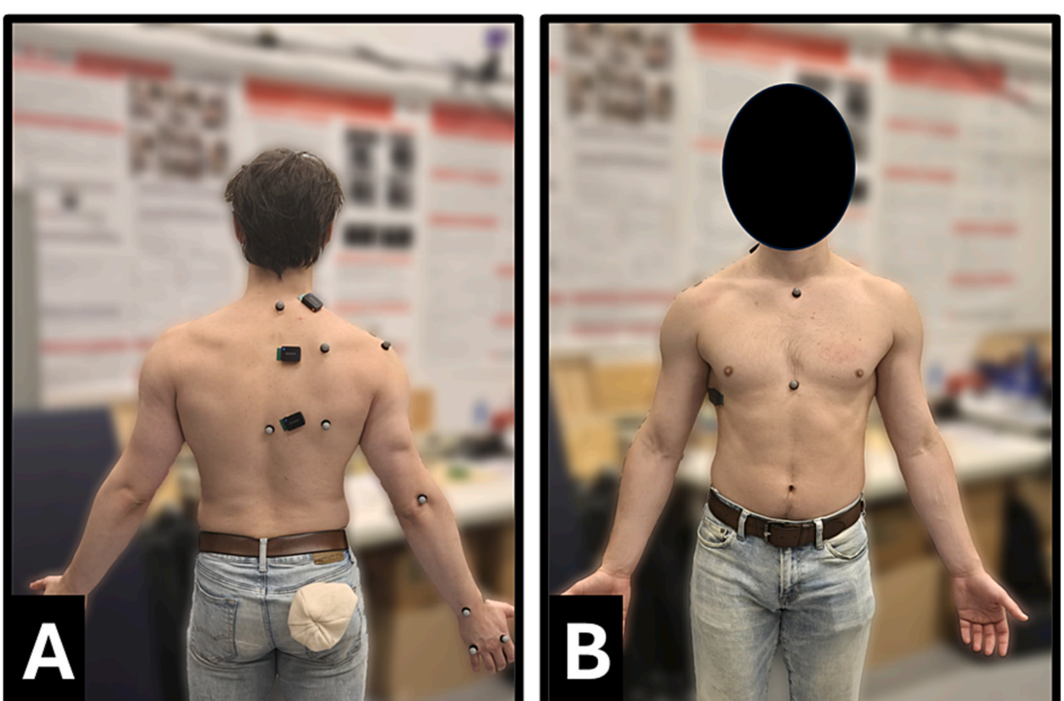

Fig. 1. Electrode and reflective marker placement from **A.** posterior, and **B.** anterior view.

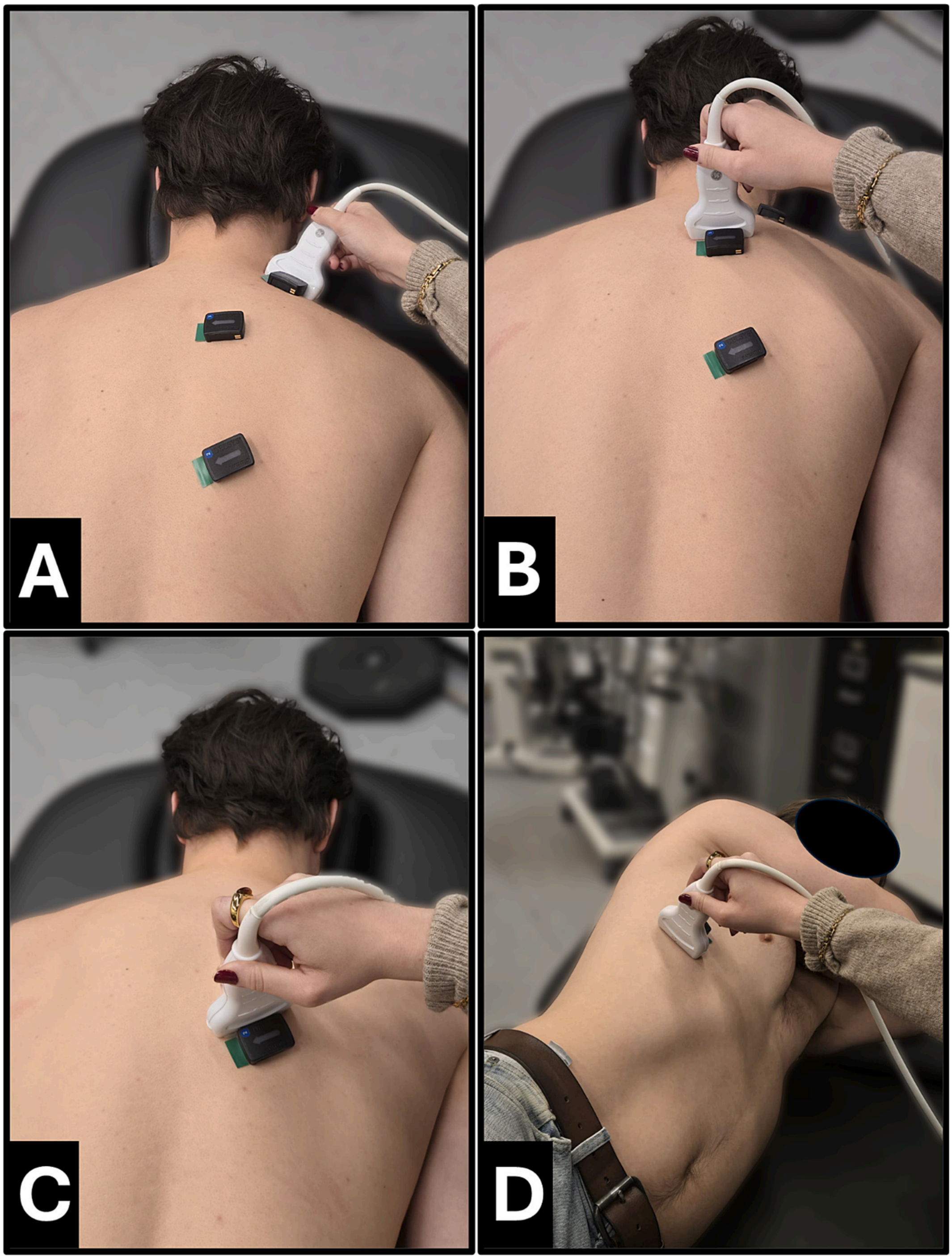

Fig. 2. Resting ultrasonographic shear wave velocity testing postures for **A.** upper trapezius **B.** middle trapezius **C.** lower trapezius and **D.** serratus anterior.

When performing ultrasonographic SWV measurements, a region of interest (ROI) was first specified from within B-mode images of each muscle taken before resting SWV. During SWV measurement, the ultrasound machine generates a low-frequency wave that propagates along the shear-axis of the underlying tissue. The ultrasound then rapidly switches to high-frequency imaging mode where it detects high-resolution tissue displacement [Cipriano et al., 2022]. Upper and lower bounds of the ROI window were set to the superficial and deep aponeuroses of the target muscle, and lateral window borders were set to maximum width. From within the bounds of the ROI, a 0.25 cm radii measurement region was automatically rectified in the centre (Fig. 3) similar to previous methods [Kelly et al., 2018; Siracusa et al., 2019]. A pilot study involving five male (27.2 ± 4.0 y; 25.5 ± 1.5 kg/m^2) and five female (24.8 ± 2.2 y; 20.0 ± 1.6 kg/m^2) participants who went on to participate in the full study were used to assess the minimum measurement region bounds representative of the participant sample of interest.

2.2.3. *Manual muscle force testing*

Muscle force for all maximal voluntary isometric contractions (MVIC) and submaximal voluntary isometric contractions (SVIC) tests (Fig. 4; Table 1) was captured using a Biodex System 4 Quickset isokinetic dynamometer (Atlas Médic Inc, Saint-Augustin-de-Desmaures, QC, Canada).

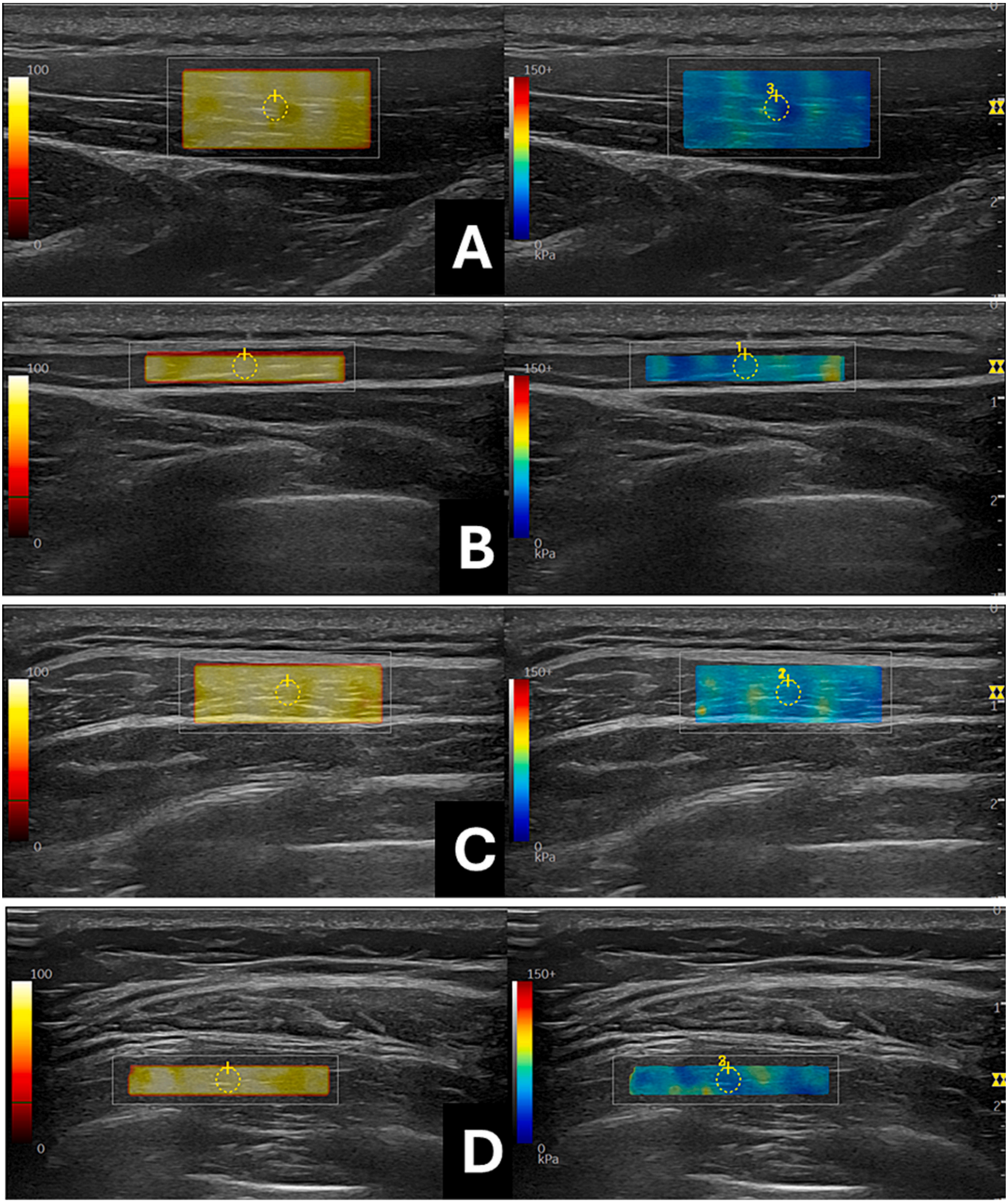

Fig. 3. Ultrasonographic shear wave elastogram visualization for **A.** upper trapezius **B.** middle trapezius **C.** lower trapezius and **D.** serratus anterior. The left-side overlay visually indicates tissue strain; regions in red are advised as unreliable for SWE. The right-side overlay visually indicates SWE from 0 kPA (dark blue) to 150 kPa (dark red). (For interpretation of the references to colour in this figure legend, the reader is referred to the web version of this article.)

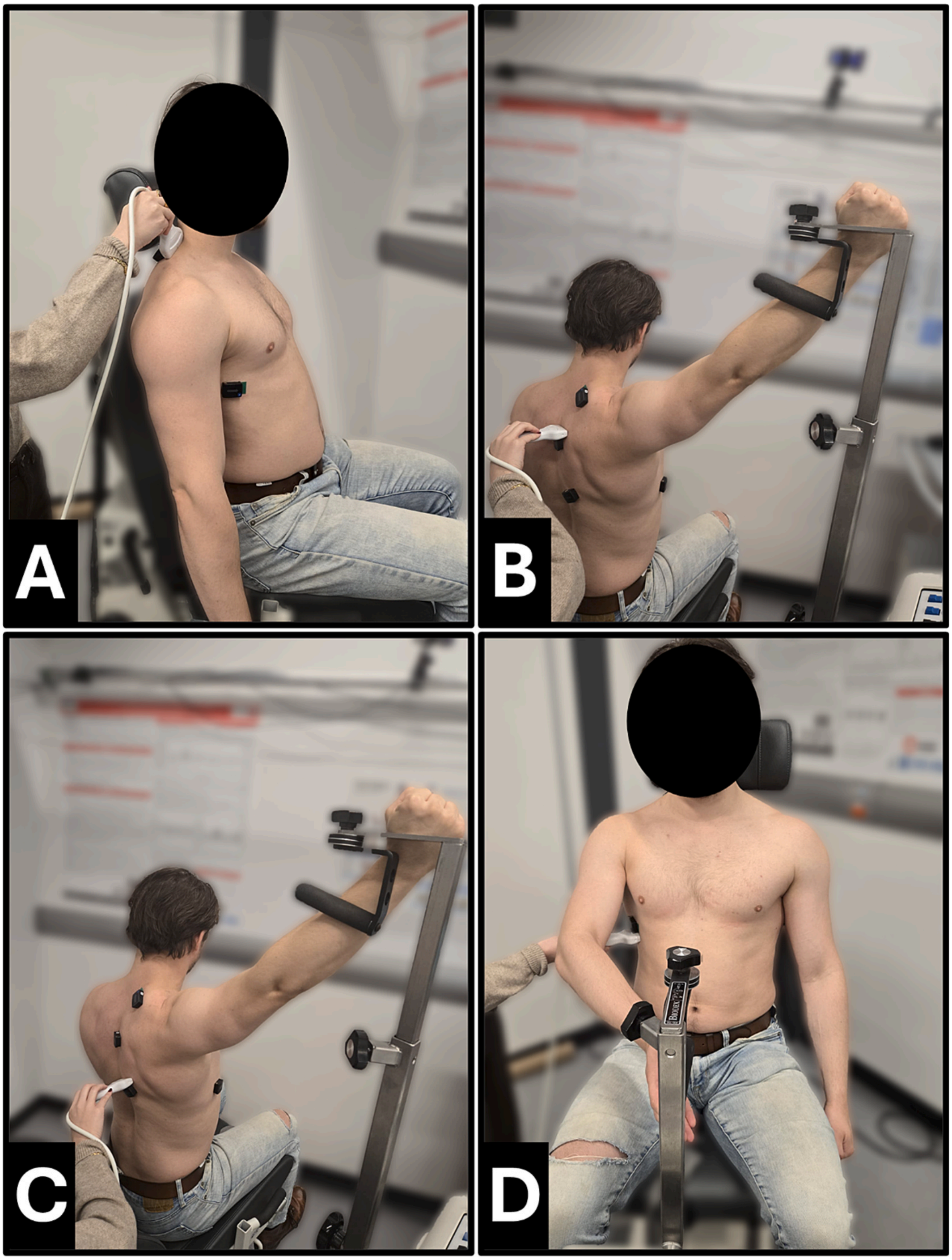

Fig. 4. MVIC and SVIC testing postures for **A.** shrug test (upper trapezius) **B.** modified prone elevation test (middle trapezius) **C.** modified prone elevation test (lower trapezius) and **D.** palm press test (serratus anterior). Ultrasound transducer placements during SVIC testing are illustrated.

2.2.4. Kinematic motion capture

Motion capture was collected using an 8-camera Vicon Vero system (Vicon Motion Systems Ltd., 7388 S. Revere Pkwy, CO, USA). Landmarking of the right upper-limb followed the recommendations by the International Society of Biomechanics (ISB) [Wu et al., 2005] (Fig. 5). Before each static scapulothoracic kinematic trial in the scapular plane described in section 2.3.1. (four pre-fatigue, four post-fatigue), participants were first instructed to hold a pole with their hand height measured in advance to produce the desired thoracohumeral elevation angle (30°, 60°, 90°, 120°). While holding the desired height, the researcher manually palpated all three scapular landmarks (inferior angle, acromion angle, trigonum spinae) and affixed 19 mm Vicon pearl markers. This process was repeated to re-localize the scapular markers immediately before each static arm elevation trial at the same arm position to attempt to control for scapular movement artefact below the skin.

Scapulothoracic joint angles were decomposed from marker positions following the defined axes of rotation suggested by the ISB [Wu et al., 2005]. Average scapulothoracic joint angle for each axis of motion was reported for each static elevation trial height and compared from pre-fatigue to post-fatigue.

Table 1
Description of MVIC and SVIC muscle tests. For all tests, the contralateral hand was instructed to be used to stabilize the exertion by holding a handle at seat height.

Test	Muscle	Description
Shrug	Upper Trapezius; UT	Dynamometer handle was aligned to the participant's dominant/right hand/arm, hanging at their side while seated (Fig. 6A). Participant was instructed to attempt to bring their shoulder to their ear (shrug) against immovable resistance [Ekstrom et al., 2005; Boettcher et al., 2008].
Modified Prone Elevation	Middle Trapezius; MT Lower Trapezius; LT	Dynamometer arm was set to vertical, and the handle was set to align with the middle of the forearm while the participant seated with their dominant/right arm in a posture of 120° thoracohumeral elevation, 0° thoracohumeral elevation, palm facing forward (Fig. 6B and 6C). Participants were instructed to push their arm backwards into the dynamometer handle supplying immovable resistance. This test was shown to be highly reliable for both MT and LT muscle recruitment [Ekstrom et al., 2005].
Palm Press	Serratus Anterior; SA	Dynamometer handle was oriented at the height of the participants navel, in line with their sagittal plane, 20 cm in front of them (Fig. 6C). The participant, seated, was instructed to press the handle towards the left side of their body against immovable resistance [Boettcher et al., 2008; Ginn et al., 2011; McDonald et al., 2017].

2.3. Protocol

2.3.1. Pre-fatigue testing

Participants were asked to remove their shirt (male) or change into a sports bra (female). Participants then laid prone on a plinth while the researcher captured resting muscle SWV of UT, MT, LT, and SA in a randomized order. Following application of surface EMG electrodes, participants resting muscle activity was recorded. Next, peak muscle force was sampled across two repetitions of MVICs for three muscle tests presented in a random order: shrug (targeting UT), modified prone elevation (targeting MT & LT), and palm press (targeting SA) [Ekstrom et al., 2005; Boettcher et al., 2008; Ginn et al., 2011; McDonald et al., 2017]. MVICs were used to scale a randomly-ordered bout of SVICs consisting of the same three muscle tests completed at 30%, 50%, and 70% MVIC force output. Participants then completed static arm elevation trials by holding their arm at 30°, 60°, 90°, and 120° thoracohumeral elevation in the scapular plane (40° anterior to frontal plane) for five seconds while holding a one kg weight [Ekstrom et al., 2004; Phadke et al., 2009]. The order of these four arm elevation trials was randomized.

2.3.2. Fatigue protocol

Participants then began a scapular muscle fatigue protocol adapted from Suzuki and colleagues [Suzuki et al., 2006]. This protocol required participants to perform four muscle tests successively, each for one minute, until they failed to maintain the proper form on three of the four tests (Fig. 6; Table 2). All tests were completed at a frequency of 30 bpm (0.5 Hz). Failure criteria for each test was determined as an inability to maintain full range of motion or 30 bpm after a single warning from the researcher. Once a muscle test reached failure, the participant immediately proceeded to the next muscle test in the protocol. If the participant completed a full cycle successfully for at least three muscle tests, they performed all muscle tests again until failure or for one minute each, whichever occurred first. An initial pilot analysis of three males (25.0 ± 1 y; 26.1 ± 1.0 kg/m^2) and three females (24.7 ± 2.9 y; 20.4 ± 1.3 kg/m^2) found that this fatigue protocol reliably induced significant group-wise increases in EMG RMS amplitude and decreases in EMG MdPF of $\geq$ 8% across UT, MT, LT, and SA, where other fatigue protocols tested from literature were unsuccessful [McQuade et al., 1998; Szucs et al., 2009; Noguchi et al., 2013].

2.3.3. Post-fatigue tests

After completing the muscle fatigue protocol, participants immediately reperformed the four static thoracohumeral elevation tasks in randomized order with a 1 kg hand load. Participants then proceeded to have their resting SWV re-assessed for UT, MT, LT, and SA. Finally, participants completed 15 isometric muscle tests consisting of the 12 SVIC tests and three MVIC tests.

2.4. Data analysis

2.4.1. Surface electromyography

EMG signals were decomposed into two metrics: root-mean-squared (RMS) amplitude, and median-power frequency (MdPF). To characterize RMS amplitude, all raw signals were first dual-band-pass filtered at 30–450 Hz [Stulen et al., 1981; Öberg, 1995; Willigenburg et al., 2012]. Peak amplitude was acquired from the middle 3-seconds of each 5-second MVIC and SVIC contraction, which was debiased and normalized to MVIC EMG RMS peak amplitude. To decompose EMG signals into

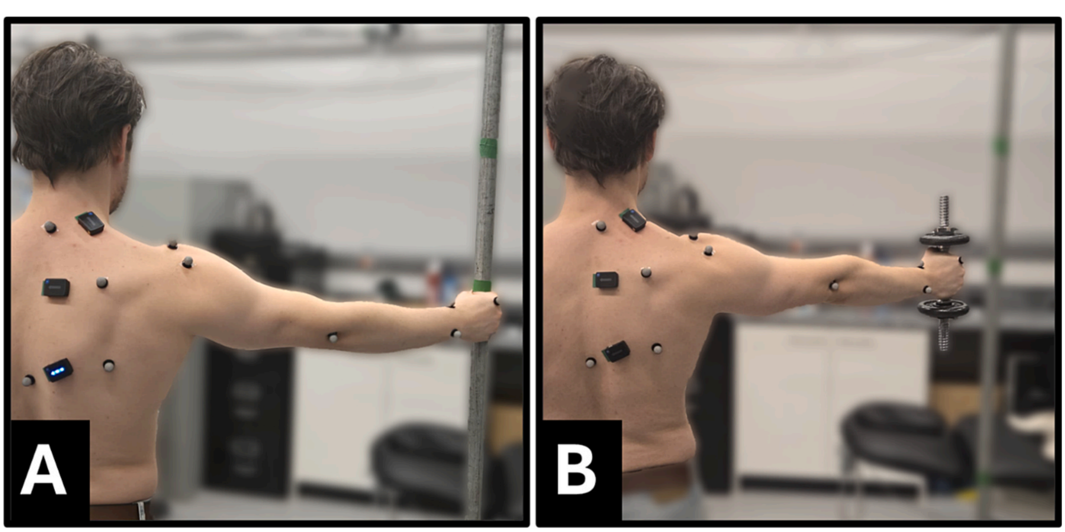

Fig. 5. Static arm elevation trial. **A.** static pole hold at 90° thoracohumeral elevation. **B.** static arm elevation with 1 kg manual load at 90° thoracohumeral elevation.

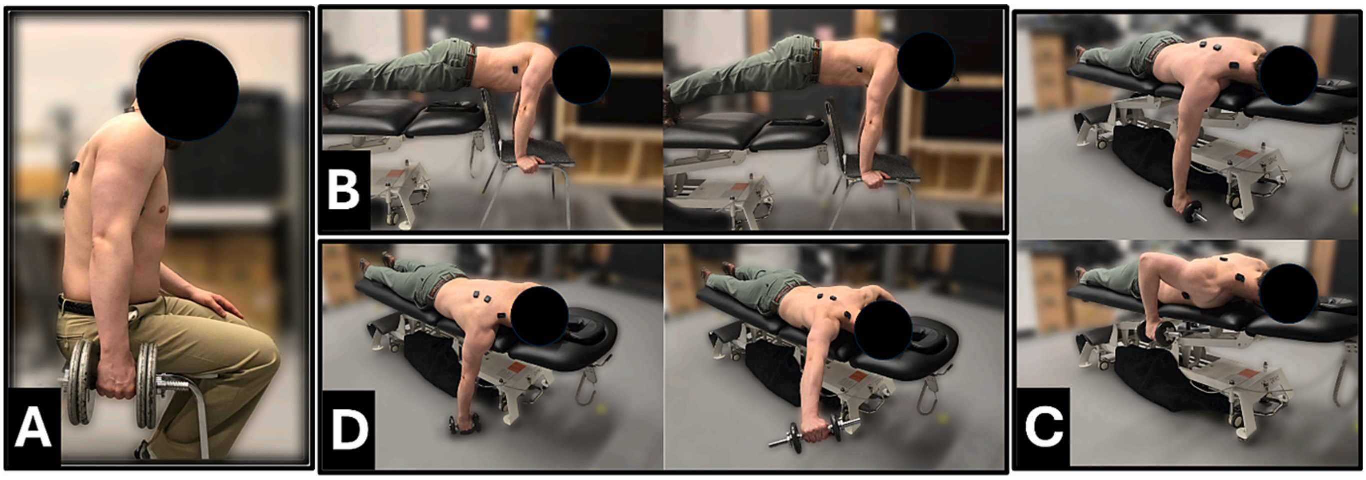

Fig. 6. Illustration of fatigue protocol tasks. **A.** shrug. **B.** push-up plus. **C.** row. **D.** prone elevation.

Table 2
Description of muscle tests used in fatigue protocol. Tests are presented in descending order as they were ordered for participants.

Test	Task Description (within two second cadence)
Shrug	Participants were instructed to raise their shoulder to their ear and return while holding load equivalent to 70% of their maximal shrug force while seated [Suzuki et al., 2006; Boettcher et al., 2008].
Push-up Plus	Participants were instructed to perform max range scapular protraction and retraction while their feet were elevated 23 cm on a height-adjustable plinth [Suzuki et al., 2006; Szucs et al., 2009].
Prone Row	Participants were instructed to lift a load equivalent to 20% of their maximal row force from a posture of 90° shoulder elevation and 0° elbow flexion to and posture of 0° shoulder elevation and 90° elbow flexion and return while prone [Suzuki et al., 2006; Noguchi et al., 2013].
Prone Elevation at 120°	Participants were instructed to raise a load equivalent to 30% of their maximal prone elevation force from a posture of 90° thoracohumeral elevation and 90° thoracohumeral plane of elevation to a posture of elevation force from a posture of 120° thoracohumeral elevation and 0° thoracohumeral plane of elevation and return while maintaining a straight elbow [Suzuki et al., 2006; Boettcher et al., 2008].

MdPF, all raw signals were first dual-band-pass filtered at 10–450 Hz [Stulen et al., 1981; Öberg, 1995; Willigenburg et al., 2012]. Signals were subsequently divided into 0.5-second epochs and filtered with a discrete Fourier transform to calculate the MdPF across the first 3-seconds of all MVIC and SVIC trials. Muscle-specific fatigue was defined as a MdPF reduction of 8% or more [Öberg, 1995].

2.4.2. Ultrasonographic shear-wave velocity

Like EMG amplitude normalization techniques, the relationship between SWV and muscle force mediated by maximal force-generating capacity may highlight the need to normalize SWV measures as a percent change in SWV relative to 0% and 100% MVC to enable comparisons between individuals [Mendes et al., 2018; Kozinc and Šarabon, 2020]. Thus, during pre-fatigue and post-fatigue resting SWV trials, SWV was calculated as the mean measure captured across seven successive SWV scans [Hatta et al., 2014; Siracusa et al., 2019; Vanhaezebrouck, 2021; Vatovec et al., 2022]. During pre-fatigue and post-fatigue SVIC muscle testing (30%, 50%, and 70% MVIC), the five second contraction window permitted two full SWV scans, from which the average was taken. SVIC SWV values were normalized as a ratio of each participants' resting SWV for each muscle [Eq. (1)].

$$normalized\,SWV = \left(\frac{Submaximal\,SWV\,(m/s)}{Resting\,SWV\,(m/s)}\right)*100 \quad (1)$$

2.4.3. Kinematic joint angles

Static scapulothoracic Euler angles were decomposed from marker positions following the Y-X-Z sequence recommended by the ISB [Wu et al., 2005]. Kinematic marker data was dual-low-pass Butterworth filtered at 6 HZ, and joint angles were calculated as the average Euler angle for each scapulothoracic DOF across the middle 2.5–3.5 s interval of each 5-second static arm hold.

2.5. Statistical analysis

For all statistical modelling, EMG RMS and MdPF, force output, SWV, and kinematic joint angle parameters all had outliers beyond two standard deviations and all pairwise data removed before analysis. However, removed data was often from the same participants, thus 5% of the kinematics data, 7% of the EMG RMS amplitude data, 3% of the EMG MdPF data and 6% of the maximal force output data was removed. One participant had outliers and pairwise measures removed for RMS, MdPF, and SWV data, thus they were also removed from the force and kinematic analysis.

To determine the effect of fatigue on maximal and submaximal SWV changes, two-way repeated measures ANOVA models compared the change in relative SWV from pre-fatigue to post-fatigue (post-fatigue minus pre-fatigue) as the dependent variable across *muscle* (upper trapezius, middle trapezius, lower trapezius, serratus anterior) and *intensity* (0% rest, 30%, 50%, and 70% force output) factors. Two additional two-way repeated measures ANOVA models were also computed to compare the change in relative EMG RMS from pre-fatigue to post-fatigue (post − pre), and relative EMG MdPF ([[post/pre]-1]*100). MdPF was presented as a ratio from baseline to easily identify post-fatigue changes which exceed a decrease of 8% used to identify myoelectric fatigue [Öberg, 1995]. 95% confidence intervals were reported with Sidak adjustments for significant effects. Mauchly sphericity tests and Omega-squared effect sizes were reported for all factors. Lastly, three paired t tests compared groupwise changes in MVIC force output as the dependent variable by muscle test (shrug, modified prone elevation, and palm press).

To determine fatigue-related neuromuscular and viscoelastic muscle tissue changes that predict scapulothoracic kinematics changes, 48 multiple regression models were computed using fatigue-related changes in EMG RMS, EMG MdPF, SWV of each muscle (UT, MT, LT, SA), and force as predictor variables and one scapulothoracic DOF (posterior tilt, medial rotation, protraction) at one angle of thoracohumeral elevation (30°, 60°, 90°, 120°) as the model dependent variable. To control for model overfitting, the contraction intensity deemed most sensitive to fatigue-related changes for each predictor variable was determined *post hoc* and selected for assignment to the regression: 100% MVIC for EMG MdPF and EMF RMS variables, and 30% SVIC for SWV. Force decrement was only captured at MVIC.

3. Results

3.1. Fatigue-related changes

ANOVA revealed significant changes in SWV associated with muscle ($F_{(3,44)} = 4.76$, $p \leq 0.001$, $\omega^2 = 0.03$; $X^2(5) = 6.120$, $p = 0.295$) and contraction intensity ($F_{(3,44)} = 58.91$, $p \leq 0.001$, $\omega^2 = 0.29$; $X^2(5) = 7.785$, $p = 0.256$) variables. Pairwise comparisons revealed a greater increase in SA SWV compared to LT, MT, and UT (Fig. 7B), and a greater increase in SWV at 30% MVIC (Fig. 7A). 50% MVIC was also significantly different from all other contraction intensities (Table 3).

ANOVA of EMG RMS amplitude change from pre-fatigue to post-fatigue indicated a significant main effect of contraction intensity ($F_{(3,43)} = 34.92$, $p \leq 0.001$, $\omega^2 = 0.01$; $X^2(5) = 9.13$, $p = 0.104$) (Fig. 8). 100% MIVC EMG RMS amplitude changes post-fatigue were significantly greater than those at submaximal intensities. However, 70% contraction intensity was still more sensitive at identifying EMG RMS amplitude increases post-fatigue than 50% (Table 4).

ANOVA modelling of EMG MdPF changes revealed a significant main effect of contraction intensity ($F_{(3,60)} = 13.38$, $p \leq 0.001$, $\omega^2 = 0.05$; $X^2(5) = 7.6$, $p = 0.13$ (Fig. 9). MdPF decrease from pre-fatigue to post-fatigue MVC was −7.1% across all muscles; 7.1% at UT, 11.1% at MT, 1.5% at LT, and 8.1% at SA. Only SA displayed a significant muscle-specific decrease that surpassed a threshold of 8% (8.1 ± 10.84; 95% CI: −13.6—0.33]) (Table 5). While MT displayed an average MdPF reduction of 11.1%, this was not significant at $\alpha = 0.05$ due to the distribution of the data.

Lastly, paired *t* test revealed significant post-fatigue decreases in MVIC force output for the modified prone elevation task ($t_{(56)} = 4.994$, $p \leq 0.001$), and a significant post-fatigue increase in MVIC force output for the palm press task ($t_{(28)} = -2.877$, $p = 0.035$) (Fig. 10).

3.2. Predictor relationships with scapulothoracic kinematics

Due to the significant differences observed in 30% SVIC SWV, 100% MVC EMG RMS amplitude, 100% MVC EMG MdPF, and 100% MVC force, these four variables (fatigue mediated difference in: 30% SWV, 100% RMS, 100% MdPF, 100% force) were determined *post-hoc* to be the regression predictor variables.

Table 3
95% margin confidence intervals for fatigue-related change in ultrasonic shear wave velocity; *muscle* x *intensity* interaction. Significant relationships are bolded. Confidence intervals across all muscles shown in first column, under each contraction intensity.

Contraction Intensity	UT[5.6 64.0]	MT[-13.8 62.1]	LT[-18.4 66.3]	SA[16.8 79.2]
0[-11.7 6.6]	[-19.7 18.1]	**[-36.7—0.3]**	**[-37.6—1.9]**	**[10.8 47.2]**
30[82.7 110.9]	**[50.4 86.8]**	**[47.6 94.0]**	**[44.3 80.7]**	**[62.3 98.7]**
50[38.9 57.1]	**[17.9 54.3]**	**[17.8 54.9]**	**[16.5 52.3]**	**[27.0 63.4]**
70 [−10.4 7.9]	[−23.0 12.4]	[-20.0 16.4]	[-25.7 10.1]	[-9.7 28.1]

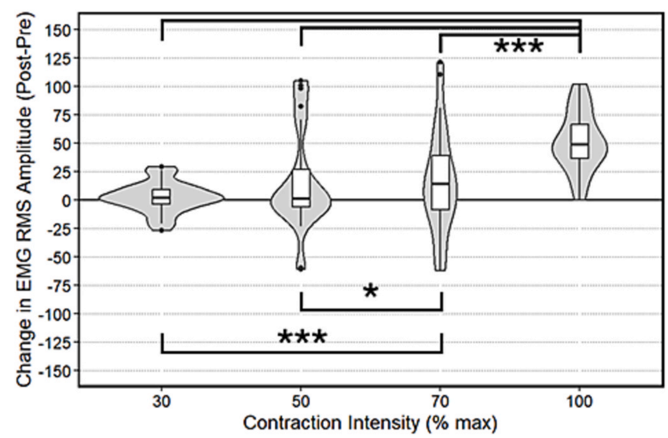

Fig. 8. Fatigue-Related change in electromyographic root-mean-squared amplitude (ordinate), grouped by contraction intensity (abscissa). Muscle factor grouped. * indicates significance at p ≤ 0.05, *** indicates significance at p ≤ 0.001.

When all predictors (fatigue mediated difference in: 30% SWV, 100% RMS, 100% MdPF, 100% force) were regressed to scapulothoracic kinematics, one significant regression model was apparent at 60° thoracohumeral elevation, two at 90° thoracohumeral elevation, and three models were apparent at 120° (Table 6). Across all six significant models, EMG MdPF was always a significant predictor variable.

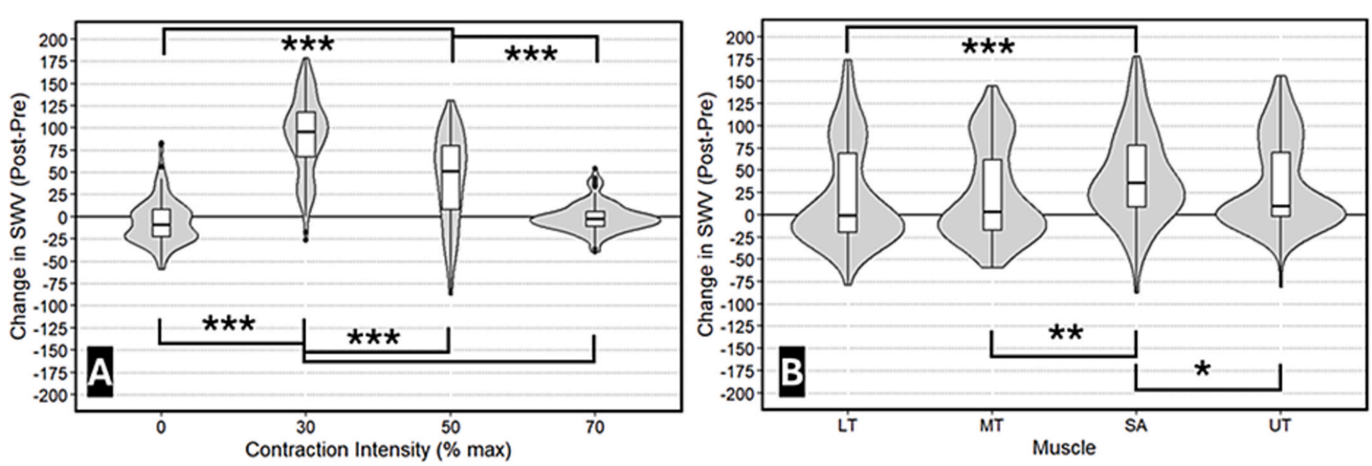

Fig. 7. Fatigue-related change in ultrasonic shear wave velocity (ordinate); grouped by muscle, separated by contraction intensity (panel **A**), and grouped by contraction intensity, separated by muscle (panel **B**). * indicates significance at p ≤ 0.05, ** indicates significance at p ≤ 0.01, *** indicates significance at p ≤ 0.001.

Table 4
95% margin confidence intervals for fatigue-related change in electromyographic root-mean-squared amplitude; *muscle* x *intensity* interaction. Significant relationships are bolded. Confidence intervals across all muscles shown in first column, under each contraction intensity.

Contraction Intensity	UT	MT	LT	SA
30[-10.4 9.3]	[-13.8 25.0]	[-27.2 18.6]	[-29.5 10.1]	[-16.0 21.2]
50[0.9 20.3]	[-3.9 35.7]	[–32.4 11.0]	**[3.2 41.1]**	**[2.0 40.0]**
70[6.4 35.2]	**[12.2 50.2]**	[-2.8 38.6]	**[12.7 49.2]**	**[7.7 47.2]**
100[41.1 60.3]	**[52.0 91.6]**	**[42.6 82.2]**	**[58.5 98.9]**	**[35.3 73.3]**

4. Discussion

The purposes of this study were to determine (1) whether changes in muscle stiffness would be spurred by a muscle fatigue task and (2) if stiffness changes and other common indices of fatigue (EMG RMS, EMG MdPF, force) would explain scapulothoracic kinematics changes. First, we hypothesized that SWV estimates of muscle stiffness would decrease following a targeted muscle fatigue task. Contrary to these expectations, increases in muscle SWV were identified at submaximal ($\geq$ 50% SVIC) contraction intensities which can be identified by the lower bound 95% confidence intervals at 30% [82.7, 110.9] and 50% [38.9, 57.1] contraction intensity. Second, we hypothesized that SWV would be a significant predictor of fatigue-related kinematics changes. Overall EMG MdPF appeared to be the strongest predictor of fatigue-related kinematics changes, yet SWV appeared to significantly predict kinematics changes in three of the six significant models, while RMS and force only found significance in two models.

4.1. Fatigue measures: ultrasonographic shear wave velocity

Regarding the literature on muscle stiffness changes with fatigue, there appears to be no current standard for muscle contraction stimulus (isometric, concentric, eccentric). The present study utilized a fatigue task consisting of alternating concentric and eccentric contractions based on previously recommended tasks in literature [McQuade et al., 1998; Suzuki et al., 2006; Szucs et al., 2009; Noguchi et al., 2013] and similar to the methods reported by one previous study investigating hamstring stiffness changes following fatiguing exercise [Vanhaezebrouck, 2021]. However, Vatovec and colleagues previously used an isometric lumbar extension fatigue protocol and Siracusa and colleagues used repeated bouts of 5-second isometric knee extension contractions. Both the studies identified post-exercise decreases in shear elastic modulus [Siracusa et al., 2019; Vatovec et al., 2022]. These studies and the theory that mechanical creep would drive stiffness decreases informed our hypothesis that resting SWV would decrease, yet this was rejected in light of SWV increases at 30% and 50% submaximal contraction intensities. One study also utilized only a purely eccentric exercise protocol, reporting increases in resting SWV of the elbow flexor muscle group were reported 15 min following targeted eccentric resistance exercise, which lasted up to 72 h before returning to baseline [Agten et al., 2017]. Chiefly, these fatigue-mediated stiffness findings from eccentric exercise contrast the stiffness decreases reported following isometric protocols. Increases in SWV post exercise were reported to have a strong correlation with Apparent Diffusion Coefficient (ADC) ($r = 0.92$, $p = 0.028$), which supports post-exercise edema and muscle perfusion as a hypothesized pathway for stiffness increases [Agten et al., 2017]. Taken together with our current findings, this may suggest that isometric exercises are likely to induce stiffness decreases,

Table 5
95% margin confidence intervals for fatigue-related change in electromyographic median-power frequency; *muscle* x *intensity* interaction. Significant decreases are bolded. Confidence intervals across all muscles shown in first column, under each contraction intensity.

Contraction Intensity	UT	MT	LT	SA
30[98.1 110.9]	[96.4 116.9]	[82.2 131.2]	[88.4 118.1]	[94.3 108.5]
50[98.8 110.0]	[87.1 120.8]	[87.9 141.6]	[93.5 109.8]	[90.0 104.6]
70[98.8 112.2]	[93.8 114.8]	[78.0 134.9]	[94.7 119.8]	[93.5 114.8]
100[89.1 97.3]	[81.2 103.0]	[71.2 106.8]	[86.8 110.3]	**[86.4 99.7]**

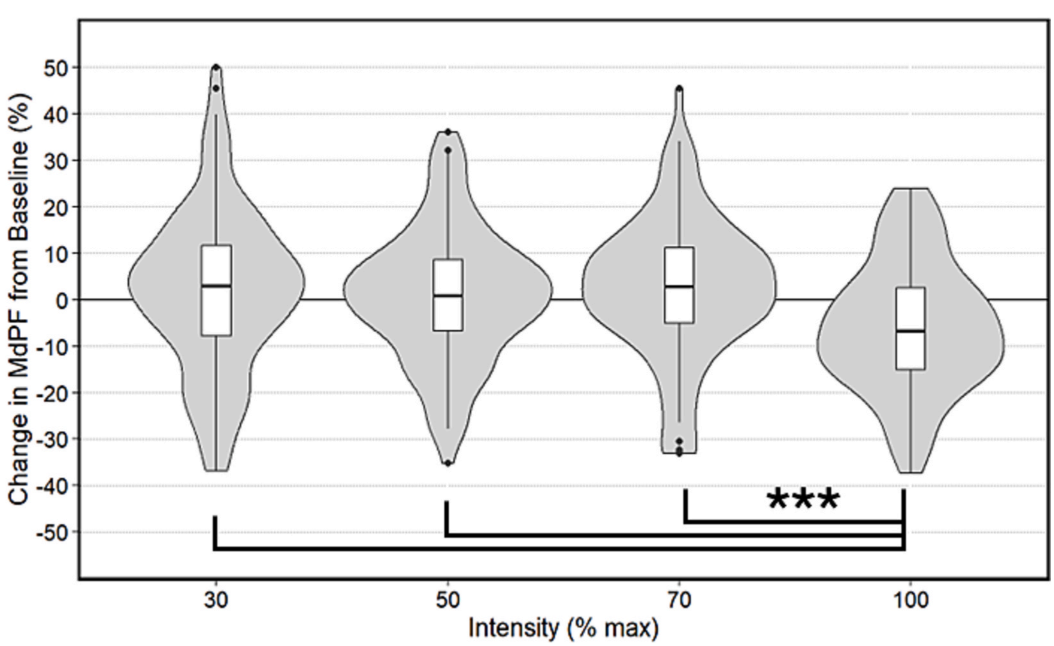

Fig. 9. Fatigue-related change in electromyographic median-power-frequency (ordinate), separated by muscle (panel) and contraction intensity (abscissa). * indicates significance at $p \leq 0.05$, *** indicates significance at $p \leq 0.001$.

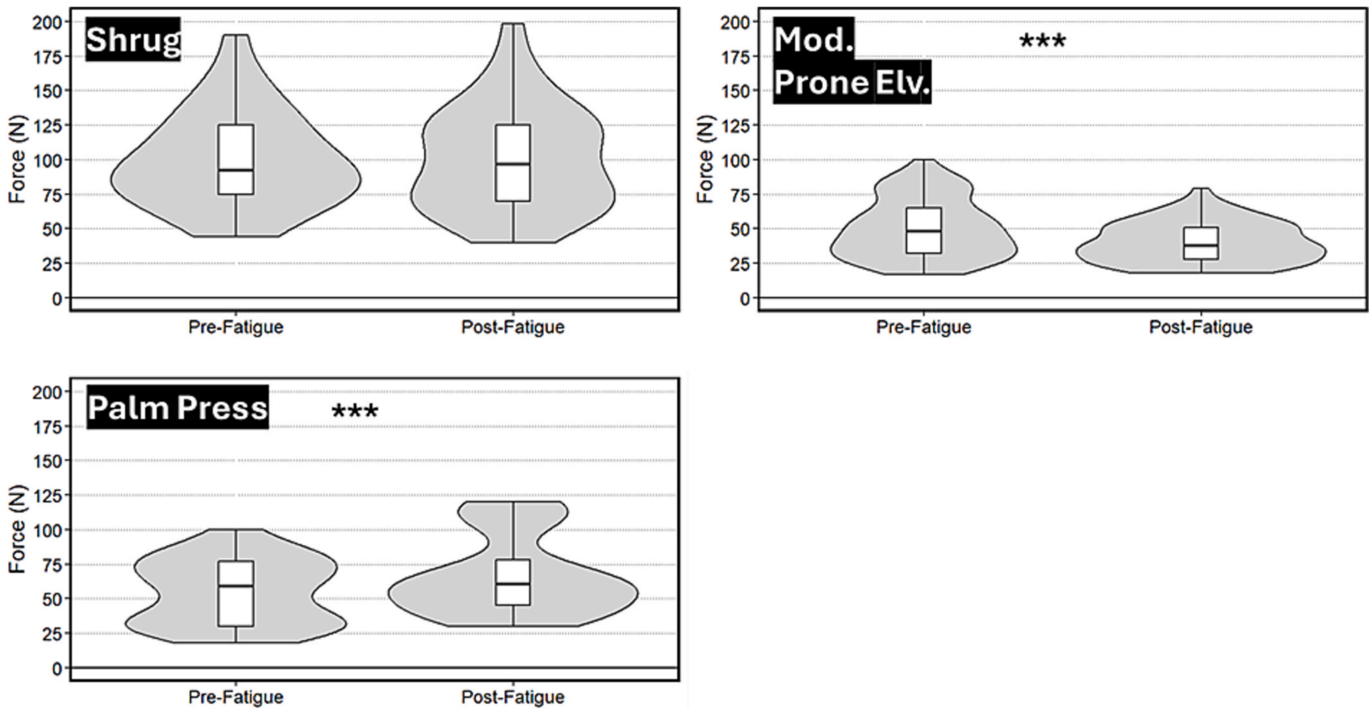

Fig. 10. Fatigue-related change in maximal voluntary isometric contraction force generating capacity (ordinate), separated by muscle (panel). *** indicates significance at $p \leq 0.001$.

while concentric and eccentric stimuli may induce stiffness increases. Since isometric contractions subject the muscle to a constant length, this may produce longer time-dependent loading characteristics compared to concentric and eccentric contractions. This may reduce the amount of energy that is expelled thermally (hysteresis), thus the stress/strain rate of the muscle tissue is minimally impacted, where stress/strain is equivalent to stiffness [Hatta et al., 2014].

A second unexpected fatigue-mediated response to muscle stiffness in our study is the presentation of significant increases in SWV at 30% and 50% SVIC, but not at 0% or 70%. Literature has long established an apparent muscle force threshold of approximately 50% MVC, above which intramuscular blood vessels collapse and arrest blood flow into the muscle completely or nearly completely [Allen et al., 2008]. This further supports the hypothesis that post-exercise increases in muscle stiffness are due to muscle edema or circulatory perfusion, as any additional muscle stiffness supplied by inward diffusion would be obstructed beyond 50% MVC, explaining why no change in muscle stiffness was observed at 70% SVIC. It remains less clear why muscle stiffness at 0% MVC (rest) appeared unaffected. However competing changes in underlying viscoelastic muscle stiffness due to exercise may have obscured any additional stiffness supplied by edema/blood pressure as MT and LT SWV demonstrated decreases at 0% MVC (rest) (Table 3), which are in line with our original hypothesis [Andonian et al., 2016; Siracusa et al., 2019; Vatovec et al., 2022]. Overall, the results of this study regarding muscle SWV changes due to concentric and eccentric exercise furthers the scant literature on this topic by illustrating that submaximal contractions below 50% intensity may be sensitive to stiffness increases.

4.2. Fatigue-mediated scapulothoracic kinematics changes

Increases in scapulothoracic posterior tilt at 90° appeared mediated by RMS amplitude and SWV increases, and EMG MdPF decreases in upper trapezius (Table 6). However, for middle trapezius, increased SWV and decreases in EMG MdPF was rather associated with anterior tilting at 120°. Increases in medial rotation at 120° appeared relative to decreased EMG MdPF and force of middle trapezius and lower trapezius, while increased SWV was also significant for middle trapezius and increased RMS was also significant for lower trapezius. Finally, decreases in upper trapezius EMG MdPF appeared related to increased scapulothoracic retraction at 90°. However, these changes only appear sensitive to specific arm elevations which suggest that fatigue-mediated changes in dynamic scapulothoracic motion could be challenging to detect.

EMG MdPF appeared to be the most significant variable for predicting fatigue-mediated scapulothoracic kinematics changes, being a significant predictor in all significant multivariable regression models. Such evidence that kinematics changes are sensitive to EMG MdPF may explain why so much variability is attributable to fatigue-mediated shoulder kinematics [Chopp-Hurley et al., 2016; Russell et al., 2024]: as MdPF changes prompt kinematic adjustments that redistribute muscle stress to less fatigued synergist muscles, this adjustment could support MdPF recovery from fatigue. We propose that in a highly redundant muscular system such as the shoulder complex, the availability of numerous equivalent load-sharing strategies may make it challenging to maintain sustained contraction from a single muscle long enough to accumulate MdPF changes associated with intracellular potassium efflux before kinematics adjustments are ultimately prompted to mitigate muscle stress [Stulen and De Luca, 1981; Arendt-Nielsen and Mills, 1985]. The relationship between EMG RMS and MdPF in our data could support this theory. RMS may be a more sensitive metric to muscle fatigue stimuli, such that it emerges at submaximal and maximal intensities (70% and 100%; Fig. 8), however, it appeared to relate to kinematic changes less consistently. Alternatively, EMG MdPF may be less sensitive to fatigue stimulus such that changes were only detectable at maximal contraction, but MdPF did appear to more robustly predict kinematics changes. The context that EMG RMS may be a more sensitive, but less robust predictor of muscle fatigue and fatigue-related kinematics changes helps explain why many studies in the literature have reported more reliable fatigue-mediated changes in amplitude compared to MdPF or MPF (mean power frequency), particularly in mechanically redundant systems like the shoulder [Ebaugh et al., 2006;

Table 6
Significant predictor variables regressed to fatigue-related scapulothoracic kinematics changes. Greyed boxes indicated non-significant regression models. 30° and 60° thoracohumeral elevation angle not reported (no significant models). Regression coefficient sign (t statistic) indicates whether the predictor relationship with each kinematic DOF is positive or negative*.

Thoracohumeral Elevation Angle	60°	90°	120°
Anterior/Posterior Tilt			
Upper Trapezius		**RMS:** $t_{(4,20)} = 3.31$, $p = 0.004$ **MdPF:** $t_{(4,20)} = -2.14$, $p = 0.035$ **SWV:** $t_{(4,20)} = 3.12$, $p = 0.005$	
Middle Trapezius			**MdPF:** $t_{(4,17)} = 3.77$, $p < 0.001$ **SWV:** $t_{(4,17)} = -3.12$, $p = 0.006$
Lower Trapezius	**MdPF:** $t_{(4,20)} = -2.32$, $p = 0.039$		
Serratus Anterior			
Upward/Downward Rotation			
Upper Trapezius			
Middle Trapezius			**MdPF:** $t_{(4,17)} = -2.36$, p = 0.034S **Force:** $t_{(4,17)} = -2.41$, $p = 0.030$ **SWV:** $t_{(4,17)} = 2.15$, $p = 0.046$
Lower Trapezius			**RMS:** $t_{(4,16)} = 3.20$, $p = 0.007$ **MdPF:** $t_{(4,16)} = -3.71$, $p = 0.003$ **Force:** $t_{(4,16)} = -4.16$, $p = 0.001$
Serratus Anterior			
Internal/External Rotation			
Upper Trapezius		**MdPF:** $t_{(4,20)} = 2.50$, $p = 0.023$	
Middle Trapezius			
Lower Trapezius			
Serratus Anterior			

* Scapulothoracic DOF directionality was consistent with ISB standard (Wu et al., 2005), such that posterior tilt, downward rotation, and internal rotation are positive.

Szucs et al., 2009; Chopp et al., 2011; Noguchi et al., 2013; Russell et al., 2024].

4.3. Limitations

A number of limitations present in the current study are a result of decisions made to follow published guidelines for EMG and SWV data collection as best as possible when competing interests were presented. Since EMG measures represent a highly validated metric of fatigue confirmation, and the sensitivity of EMG placement on signal characteristics is well established [Besomi et al., 2019], the decision was made to prioritize correct EMG placement over ultrasound probe location. This resulted in transducer placements tangential to EMG electrode placement, offset from the recommended localization by approximately 2 cm but still in line with fiber orientation. Secondly, as fatigue is a transient condition that resolves with rest [Enoka and Stuart, 1992; Enoka, 1995; Enoka and Duchateau, 2008], post-fatigue EMG and force measurements may have been influenced by the 15–20 min post-fatigue collection window where kinematic, resting SWV, and submaximal EMG, force, and SWV measurements were acquired. Specifically, due to pseudo randomization or the submaximal contraction ordering for each participant, this likely provided different muscles with preferential recovery post-exercise and inflated the group-wise variability in related EMG, force, and SWV post-fatigue measures. In interpreting the submaximal SWV and EMG measures in particular, the associated risk is that this data may be subject to an inflated type II error rate (false negative), where earlier post-fatigue testing may have detected changes that did not persist to the 15–20 min window. Consequently, recovery is unlikely to have influenced an increased type I error rate (false positive), which coincides with evidence that MdPF and MPF changes beyond 8% do not reliably occur in non-fatigued muscle [Öberg, 1995], suggesting that significant findings were not artefacts of lenient testing. While measures of fatigue are expected to return to baseline with rest, literature suggests that SWV measures following similar concentric-eccentric muscle exercise persists and even continues to peak up to 72 h later [Agten et al., 2017]. Recovery effects on EMG measures fatigue do not last on the order of days, yet evidence that neuromuscular fatigue persists up to 60 min in primary agonist muscles of the shoulder following fatigue help to support our 20-minute post fatigue collection window [McDonald et al., 2016], which likely reflects sustained decreases in intracellular ion concentration [Tupling et al., 2000] and reduced central drive that is expected to last for a timescale similar to the length of the fatiguing protocol [Carroll et al., 2017]. Our intent in this study was to consolidate some of the most promising scapular stabilizer muscle fatigue protocols in literature, however UT in particular appeared to fatigue less reliably with the current protocol, thus future studies may wish to modify the current protocol with a different UT fatigue stimuli. However, it remains unclear if non-significant fatigue-mediated changes in UT force were due to failure to fatigue this muscle, load-sharing to sustain post-fatigue force output, or whether UT recovered from fatigue before post-fatigue force and EMG were captured. Lastly, with appropriate power, a weighted or regularized regression model would be more ideal than using ANOVA and *t*-test post-hoc as dimensionality reduction determinants to select variables as predictors as completed in this research. However, our sample of 8 EMG measures (RMS and MdPF; maximal and submaximal), 4 SWV measures, and force measures across 4 muscles provided more candidate predictor variables than we could robustly prescribe to a regression without risking overfitting. We acknowledge the trade-off between model stability and selection bias as a trade-off imposed by our sample size.

5. Conclusion

This study sought whether fatigue-mediated changes in muscle stiffness, measured using ultrasonographic SWV, can be utilized to assess fatigue state and predict fatigue-mediated kinematics changes prompted by load-sharing. Unexpectedly, SWV measures reliably increased during 30% and 50% submaximal contractions, indicating that SWV responses to concentric-eccentric exercise may be different than isometric exercise responses reported in literature. Regression modelling between metrics of muscle fatigue (force, EMG amplitude, EMG MdPF, SWV) and kinematics suggest that EMG MdPF may signal a threshold of sustained fatigue accumulation that prompts load-sharing changes and subsequent kinematics changes which is more robust than EMG RMS, muscle force changes, and SWV. Future research may wish to find more direct methods for testing the hypothesis that kinematics changes are prompted by fatigue-mediate changes in MdPF, such as evaluating kinematics changes during a sustained contraction in a redundant muscular system with time-synchronized EMG amplitude and EMG MdPF comparisons.

Funding Sources

This project was funded by Natural Sciences and Engineering Research Councils of Canada Discovery Grants held by each Dr. Jaclyn Hurley and Dr. Janessa Drake, and an Alexander Graham Bell Postgraduate Doctoral Scholarship held by Matthew S. Russell. Funding for the equipment used in this project was provided by the Canada Foundation for Innovation and the Ontario Research Fund.

CRediT authorship contribution statement

Matthew S. Russell: Writing – review & editing, Writing – original draft, Visualization, Methodology, Investigation, Formal analysis, Data curation, Conceptualization. **Janessa D.M. Drake:** Writing – review & editing, Supervision, Project administration, Methodology, Funding acquisition, Formal analysis, Conceptualization. **Jaclyn N. Chopp-Hurley:** Writing – review & editing, Supervision, Project administration, Methodology, Funding acquisition, Formal analysis, Conceptualization.

Declaration of competing interest

The authors declare that they have no known competing financial interests or personal relationships that could have appeared to influence the work reported in this paper.

Data availability

Data will be made available on request.

References

Agten, C.A., Buck, F.M., Dyer, L., Flück, M., Pfirrmann, C.W., Rosskopf, A.B., 2017. Delayed-onset muscle soreness: temporal assessment with quantitative MRI and shear-wave ultrasound elastography. Am. J. Roentgenol. 208 (2), 402–412.

Allen, D.G., Lamb, G.D., Westerblad, H., 2008. Skeletal muscle fatigue: cellular mechanisms. Physiol. Rev.

Andonian, P., Viallon, M., Le Goff, C., de Bourguignon, C., Tourel, C., Morel, J., Giardini, G., Gergele, L., Millet, G.P., Croisille, P., 2016. Shear-wave elastography assessments of quadriceps stiffness changes prior to, during and after prolonged exercise: a longitudinal study during an extreme mountain ultra-marathon. PLoS One 11 (8), e0161855.

Arendt-Nielsen, L., Mills, K., 1985. The relationship between mean power frequency of the EMG spectrum and muscle fibre conduction velocity. Electroencephalogr. Clin. Neurophysiol. 60 (2), 130–134.

Besomi, M., Hodges, P.W., Van Dieën, J., Carson, R.G., Clancy, E.A., Disselhorst-Klug, C., Holobar, A., Hug, F., Kiernan, M.C., Lowery, M., 2019. Consensus for experimental design in electromyography (CEDE) project: Electrode selection matrix. J. Electromyogr. Kinesiol. 48, 128–144.

Boettcher, C.E., Ginn, K.A., Cathers, I., 2008. Standard maximum isometric voluntary contraction tests for normalizing shoulder muscle EMG. J. Orthop. Res. 26 (12), 1591–1597.

Bouillard, K., Nordez, A., Hodges, P.W., Cornu, C., Hug, F., 2012. Evidence of changes in load sharing during isometric elbow flexion with ramped torque. J. Biomech. 45 (8), 1424–1429.

Bouillard, K., Nordez, A., Hug, F., 2011. Estimation of individual muscle force using elastography. PLoS One 6 (12), e29261.

Carroll, T.J., Taylor, J.L., Gandevia, S.C., 2017. Recovery of central and peripheral neuromuscular fatigue after exercise. J. Appl. Physiol. 122 (5), 1068–1076.

Chopp-Hurley, J.N., O'Neill, J.M., McDonald, A.C., Maciukiewicz, J.M., Dickerson, C.R., 2016. Fatigue-induced glenohumeral and scapulothoracic kinematic variability: implications for subacromial space reduction. J. Electromyogr. Kinesiol. 29, 55–63.

Chopp, J.N., Fischer, S.L., Dickerson, C.R., 2011. The specificity of fatiguing protocols affects scapular orientation: Implications for subacromial impingement. Clin. Biomech. 26 (1), 40–45.

Cipriano, K.J., Wickstrom, J., Glicksman, M., Hirth, L., Farrell, M., Livinski, A.A., Esfahani, S.A., Maldonado, R.J., Astrow, J., Berrigan, W.A., 2022. A scoping review of methods used in musculoskeletal soft tissue and nerve shear wave elastography studies. Clinic Neurophys 140, 181–195.

Ebaugh, D.D., McClure, P.W., Karduna, A.R., 2006. Effects of shoulder muscle fatigue caused by repetitive overhead activities on scapulothoracic and glenohumeral kinematics. J. Electromyogr. Kinesiol. 16 (3), 224–235.

Ekstrom, R.A., Bifulco, K.M., Lopau, C.J., Andersen, C.F., Gough, J.R., 2004. Comparing the function of the upper and lower parts of the serratus anterior muscle using surface electromyography. J. Orthop. Sports Phys. Ther. 34 (5), 235–243.

Ekstrom, R.A., Soderberg, G.L., Donatelli, R.A., 2005. Normalization procedures using maximum voluntary isometric contractions for the serratus anterior and trapezius muscles during surface EMG analysis. J. Electromyogr. Kinesiol. 15 (4), 418–428.

Enoka, R.M., 1995. Mechanisms of muscle fatigue: central factors and task dependency. J. Electromyogr. Kinesiol. 5 (3), 141–149.

Enoka, R.M., Duchateau, J., 2008. Muscle fatigue: what, why and how it influences muscle function. J. Physiol. 586 (1), 11–23.

Enoka, R.M., Stuart, D.G., 1992. Neurobiology of muscle fatigue. J. Appl. Physiol. 72 (5), 1631–1648.

Faul, F., Erdfelder, E., Lang, A.-G., Buchner, A., 2007. G* Power 3: a flexible statistical power analysis program for the social, behavioral, and biomedical sciences. Behav. Res. Methods 39 (2), 175–191.

Ginn, K., Halaki, M., Cathers, I., 2011. Revision of the shoulder normalization tests is required to include rhomboid major and teres major. J. Orthop. Res. 29 (12), 1846–1849.

Hatta, T., Yamamoto, N., Sano, H., Itoi, E., 2014. In vivo measurement of rotator cuff tendon strain with ultrasound elastography: an investigation using a porcine model. J. Ultrasound Med. 33 (9), 1641–1646.

Kelly, J.P., Koppenhaver, S.L., Michener, L.A., Proulx, L., Bisagni, F., Cleland, J.A., 2018. Characterization of tissue stiffness of the infraspinatus, erector spinae, and gastrocnemius muscle using ultrasound shear wave elastography and superficial mechanical deformation. J. Electromyogr. Kinesiol. 38, 73–80.

Kozinc, Ž., Šarabon, N., 2020. Shear-wave elastography for assessment of trapezius muscle stiffness: Reliability and association with low-level muscle activity. PLoS One 15 (6), e0234359.

Kubo, K., Kanehisa, H., Kawakami, Y., Fukunaga, T., 2001. Influences of repetitive muscle contractions with different modes on tendon elasticity in vivo. J. Appl. Physiol. 91 (1), 277–282.

McDonald, A.C., Sonne, M.W., Keir, P.J., 2017. Optimized maximum voluntary exertion protocol for normalizing shoulder muscle activity. International Biomechanics 4 (1), 9–16.

McDonald, A.C., Tse, C.T.F., Keir, P.J., 2016. Adaptations to isolated shoulder fatigue during simulated repetitive work. Part II: Recovery. J. Electromyogr. Kinesiol. 29, 42–49.

McQuade, K.J., Dawson, J., Smidt, G.L., 1998. Scapulothoracic muscle fatigue associated with alterations in scapulohumeral rhythm kinematics during maximum resistive shoulder elevation. J. Orthop. Sports Phys. Ther. 28 (2), 74–80.

Mendes, B., Firmino, T., Oliveira, R., Neto, T., Infante, J., Vaz, J.R., Freitas, S.R., 2018. Hamstring stiffness pattern during contraction in healthy individuals: analysis by ultrasound-based shear wave elastography. Eur. J. Appl. Physiol. 118, 2403–2415.

Noguchi, M., Chopp, J.N., Borgs, S.P., Dickerson, C.R., 2013. Scapular orientation following repetitive prone rowing: implications for potential subacromial impingement mechanisms. J. Electromyogr. Kinesiol. 23 (6), 1356–1361.

Öberg, T., 1995. Muscle fatigue and calibration of EMG measurements. J. Electromyogr. Kinesiol. 5 (4), 239–243.

Phadke, V., Camargo, P., Ludewig, P., 2009. Scapular and rotator cuff muscle activity during arm elevation: a review of normal function and alterations with shoulder impingement. Braz. J. Phys. Ther. 13, 1–9.

Russell, M.S., Vasilounis, S.S., Lefebvre, E., Drake, J.D., Chopp-Hurley, J.N., 2024. Variability in musculoskeletal fatigue responses associated with repeated exposure to an occupational overhead drilling task completed on successive days. Hum. Mov. Sci. 97, 103276.

Siracusa, J., Charlot, K., Malgoyre, A., Conort, S., Tardo-Dino, P.-E., Bourrilhon, C., Garcia-Vicencio, S., 2019. Resting muscle shear modulus measured with ultrasound shear-wave elastography as an alternative tool to assess muscle fatigue in humans. Front. Physiol. 10, 626.

Stulen, F.B., De Luca, C.J., 1981. Frequency parameters of the myoelectric signal as a measure of muscle conduction velocity. IEEE Trans. Biomed. Eng. 7, 515–523.

Suzuki, H., Swanik, K.A., Huxel, K.C., Kelly, J.D., Swanik, C.B., 2006. Alterations in upper extremity motion after scapular-muscle fatigue. J. Sport Rehabil. 15 (1), 71–88.

Szucs, K., Navalgund, A., Borstad, J.D., 2009. Scapular muscle activation and co-activation following a fatigue task. Med. Biol. Eng. Compu. 47 (5), 487–495.

Tupling, R., Green, H., Grant, S., Burnett, M., Ranney, D., 2000. Postcontractile force depression in humans is associated with an impairment in SR Ca2+ pump function. American Journal of Physiology-Regulatory, Integrative and Comparative Physiology 278 (1), R87–R94.

Vanhaezebrouck E (2021). The influence of fatigue on the hamstring muscle stiffness in adult athletes, using shear wave elastography, Ghent University.

Vatovec, R., Kozinc, Ž., Voglar, M., 2022. The Effects of Isometric Fatigue on trunk Muscle Stiffness: Implications for Shear-Wave Elastography Measurements. Sensors 22 (23), 9476.

Willigenburg, N.W., Daffertshofer, A., Kingma, I., van Dieën, J.H., 2012. Removing ECG contamination from EMG recordings: a comparison of ICA-based and other filtering procedures. J. Electromyogr. Kinesiol. 22 (3), 485–493.

Wu, G., Van der Helm, F.C., Veeger, H.D., Makhsous, M., Van Roy, P., Anglin, C., Nagels, J., Karduna, A.R., McQuade, K., Wang, X., 2005. ISB recommendation on

definitions of joint coordinate systems of various joints for the reporting of human joint motion—Part II: shoulder, elbow, wrist and hand. J. Biomech. 38 (5), 981–992.
Yoshitake, Y., Takai, Y., Kanehisa, H., Shinohara, M., 2014. Muscle shear modulus measured with ultrasound shear-wave elastography across a wide range of contraction intensity. Muscle Nerve 50 (1), 103–113.
Zimmer, M., Kleiser, B., Marquetand, J., Ateş, F., 2023. Shear wave elastography characterizes passive and active mechanical properties of biceps brachii muscle in vivo. J. Mech. Behav. Biomed. Mater. 137, 105543.